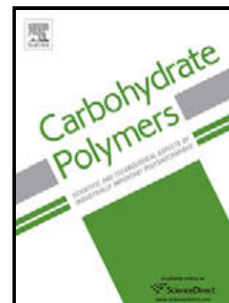


Journal Pre-proof

Conducting composite films based on chitosan or sodium hyaluronate. Properties and cytocompatibility with human induced pluripotent stem cells



Daniela Jasenská (Investigation), Věra Kašpárková (Conceptualization) (Methodology), Katarzyna Anna Radaszkiewicz (Investigation), Zdenka Capáková (Conceptualization) (Methodology) (Investigation), Jiří Pacherník (Methodology) (Investigation), Miroslava Trchová (Investigation), Antonín Minařík (Investigation), Jan Vajďák (Investigation), Tomáš Bárta (Investigation), Jaroslav Stejskal (Methodology), Marián Lehocký (Investigation), Thanh Huong Truong (Investigation), Robert Moučka (Investigation), Petr Humpolíček (Conceptualization) (Methodology)

PII: S0144-8617(20)31417-X

DOI: <https://doi.org/10.1016/j.carbpol.2020.117244>

Reference: CARP 117244

To appear in: *Carbohydrate Polymers*

Received Date: 9 April 2020

Revised Date: 24 August 2020

Accepted Date: 12 October 2020

Please cite this article as: Jasenská D, Kašpárková V, Radaszkiewicz KA, Capáková Z, Pacherník J, Trchová M, Minařík A, Vajďák J, Bárta T, Stejskal J, Lehocký M, Truong TH, Moučka R, Humpolíček P, Conducting composite films based on chitosan or sodium hyaluronate. Properties and cytocompatibility with human induced pluripotent stem cells, *Carbohydrate Polymers* (2020), doi: <https://doi.org/10.1016/j.carbpol.2020.117244>

This is a PDF file of an article that has undergone enhancements after acceptance, such as the addition of a cover page and metadata, and formatting for readability, but it is not yet the definitive version of record. This version will undergo additional copyediting, typesetting and review before it is published in its final form, but we are providing this version to give early visibility of the article. Please note that, during the production process, errors may be discovered which could affect the content, and all legal disclaimers that apply to the journal pertain.

© 2020 Published by Elsevier.

Conducting composite films based on chitosan or sodium hyaluronate. Properties and cytocompatibility with human induced pluripotent stem cells

Daniela Jasenská^a, Věra Kašpárková^a, Katarzyna Anna Radaszkiewicz^b, Zdenka Capáková^a, Jiří Pacherník^b, Miroslava Trchová^c, Antonín Minařík^a, Jan Vajdák^a, Tomáš Bárta^b, Jaroslav Stejskal^d, Marián Lehocký^a, Thanh Huang Truong^a, Robert Moučka^a, Petr Humpolíček^{a*}

^a Centre of Polymer Systems and Faculty of Technology, Tomas Bata University in Zlin, 760 01 Zlin, Czech Republic

^b Masaryk University, Faculty of Science, 625 00 Brno, Czech Republic

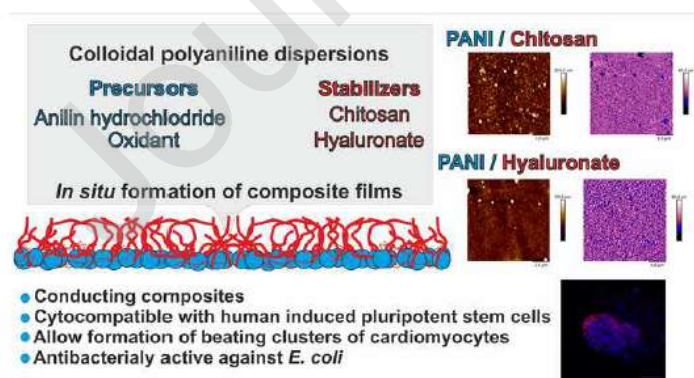
^c University of Chemistry and Technology Prague, Central Laboratories, 166 28 Prague 6, Czech Republic

^d Institute of Macromolecular Chemistry, Academy of Sciences of the Czech Republic, 162 06 Prague 6, Czech Republic

E-mails: DJ – jasenska@utb.cz; VK – vkasarkova@utb.cz; KAR – radasziewicz@sci.muni.cz; JP – jipa@sci.muni.cz; MT – trchova@imc.cas.cz; AM – minarik@utb.cz; JV – vajdak@utb.cz; TB – tbarta@med.muni.cz; JS – stejskal@imc.cas.cz; ML – lehocky@utb.cz; ZC – capakova@utb.cz; THT – truong@utb.cz; PH – humpolicek@utb.cz

* Corresponding author. E-mail: humpolicek@utb.cz, +420 576 038 035, ORCID: 0000-0002-6837-6878

Graphical abstract



Highlights

- Novel approach for preparation of PANI/polysaccharide composites was proposed.
- Conducting composites of PANI with chitosan or sodium hyaluronate were prepared.
- Composites were cytocompatible with human induced pluripotent stem cells.
- Composites exhibited antibacterial activity.

Abstract

Novel composite films combining biocompatible polysaccharides with conducting polyaniline (PANI) were prepared *via* the *in-situ* polymerization of aniline hydrochloride in the presence of sodium hyaluronate (SH) or chitosan (CH). The composite films possess very good cytocompatibility in terms of adhesion and proliferation of two lines of human induced pluripotent stem cells (hiPSC). Moreover, the cardiomyogenesis and even formation of beating clusters were successfully induced on the films. The proportion of formed cardiomyocytes demonstrated excellent properties of composites for tissue engineering of stimuli-responsive tissues. The testing also demonstrated antibacterial activity of the films against *E. coli* and PANI-SH was able to reduce bacterial growth from 2×10^5 to < 1 cfu cm^{-2} . Physicochemical characterization revealed that the presence of polysaccharides did not notably influence conductivities of the composites being ~ 1 and ~ 2 S cm^{-1} for PANI-SH and PANI-CH respectively; however, in comparison with neat PANI, it modified their topography making the films smoother with mean surface roughness of 4 (PANI-SH) and 14 nm (PANI-CH). The combination of conductivity, antibacterial activity and mainly cytocompatibility with hiPSC opens wide application potential of these polysaccharide-based composites.

Keywords: polyaniline, polysaccharides; conducting composites; human induced pluripotent stem cells;

1. Introduction

Combinations of bioactive polysaccharides with conducting polymers gives rise to promising materials with versatile applications and interesting properties. Here, chitosan/PANI hydrogels for biosensors (Uluturk & Alemdar, 2018), flexible chitosan/PANI films with good mechanical properties (Thanpitcha, Sirivat, Jamieson, & Rujiravanit, 2006) or gamma- Fe_2O_3 /chitosan/PANI nanocomposites for adsorption of deoxyribonucleic acid (Maciel et al., 2018) can be mentioned as examples.

Among conducting polymers, polyaniline (PANI) is at the centre of attention thanks to its easy synthesis, stability, reasonably high conductivity, unique redox characteristics (Qin, Tao, & Yang, 2010; Stejskal & Sapurina, 2005; Stejskal, Sapurina, & Trchova, 2010), and intrinsic electronic and ionic conductivity (Paulsen, Tybrandt, Stavrinidou, & Rivnay, 2020), which are all advantageous for biomedical applications (Liu et al., 2020; Zare et al., 2020). PANI may also be prepared in various forms – powders, thin films or colloidal dispersions. ~~The basic synthesis of PANI powders has previously been described by. However, the powder is insoluble in common organic solvents and is difficult to process. To avoid this shortcoming~~ However, for application in biological systems, aqueous colloidal dispersions are the most interesting forms of PANI. They are prepared *via* aniline polymerization in the presence of a steric stabilizer, ~~which produces a colloidal PANI in the form of an aqueous dispersion~~ (Stejskal & Sapurina, 2005). Commonly, water-soluble synthetic polymers or surfactants can be used as stabilizers; nevertheless, only a few biomacromolecules, such as cellulose derivatives (Chattopadhyay, Banerjee, Chakravorty, & Mandal, 1998; Stejskal, Spirkova, et al., 1999) or gelatin (Bober et al., 2017), have been exploited for the synthesis of colloidal PANI. For materials coming into contact with cells and tissues, polysaccharides such as sodium hyaluronate and chitosan appear to be excellent candidates as stabilizers due to their good environmental, and especially, biological properties (Kasparkova et al., 2019). From the dialyzed colloidal dispersions, composite films can be simply cast, followed by evaporation of water.

The present study uses alternative strategy for the preparation of thin PANI films consisting in coating of surfaces *in situ* during the preparation of PANI colloids. In general, any surface in contact with the reaction mixture used for PANI synthesis becomes coated with a thin PANI film of submicrometer thickness (Stejskal & Sapurina, 2005; Stejskal, Sapurina, Prokes, & Zemek, 1999). The PANI films are also produced on surfaces immersed to PANI colloidal dispersions containing water-soluble polymer stabilizers (Riede, Helmstedt, Riede, Zemek, & Stejskal, 2000) (Riede, Helmstedt, Sapurina, & Stejskal, 2002). In the literature, however, *in-situ* prepared composite films deposited during the preparation of colloidal dispersions of PANI and polysaccharides have not previously been investigated. ~~In this regard, attention has recently been turned to colloidal PANI dispersions stabilized with bioactive sodium hyaluronate and chitosan.~~

Glycosaminoglycan sodium hyaluronate (SH) is present in the extracellular matrix, synovial fluid, soft connective tissues, skin, lungs and muscle tissues (Wnek, 2004). It is

composed of repeating disaccharide units of D-glucuronic acid and *N*-acetyl-D-glucosamine (Lapcik, De Smedt, Demeester, & Chabreck, 1998). Hyaluronate is a biocompatible, biodegradable, and non-immunogenic biomaterial that finds numerous biomedical applications (Hu, Sabelman, Tsai, Tan, & Hentz, 2000; Kirker, Luo, Nielson, Shelby, & Prestwich, 2002). The second used polysaccharide, chitosan, is a cationic polyelectrolyte of β -[1,4]-linked 2-acetamido-2-deoxy-D-glucopyranose and 2-amino-2-deoxy-D-glucopyranose, which is obtained by the deacetylation of chitin. Correspondingly to SH, this polysaccharide has unique characteristics, such as biodegradability and biocompatibility; moreover, it shows antimicrobial (Ozkan & Sasmazel, 2018) and antioxidant properties. Interestingly, it has been recently reported that chitin, which is a source for chitosan production, showed biocompatibility with different cell types, including cardiomyocytes differentiated from induced pluripotent stem cells (hiPSCs) (Machalowski et al., 2019) which are also used in our study. HiPSCs are namely at the centre of attention with respect to their unique properties, such as self-renewal capacity and especially ability to differentiate into any cell type of the human body. Their discovery hence opened up new opportunities in the biomedical sciences (Fernandez, Fernandez, & Mencialha, 2013).

~~Considering the vast amount of new possibilities conducting polymers offer~~ In this study, we aim to prepare novel conducting composite films on immersed supports *in-situ* during the formation of colloidal PANI dispersions containing sodium hyaluronate or chitosan as steric stabilizers. The novelty of the research presented here relies not only in the unique combination of biocompatible polysaccharides and synthetic conducting polymers in composite films, but also in the complementary and thorough characterization of their biological properties when in contact with prospective cell line, hiPSC. The comprehensive physico-chemical characteristics (conductivity, surface characteristics, interfacial behaviour) of the prepared composites serve as a basis for deeper understanding of the cell behaviour on these surfaces, enabling trouble-free contact with cells with simultaneous stimuli responsivity provided by conducting PANI.

2. Experimental

2.1. Materials

Chitosan (CH; average molecular weight $\sim 4 \times 10^5$, deacetylation degree higher than 75 %) was purchased from Sigma Aldrich (Germany). Sodium hyaluronate (SH; molecular weight $1-1.5 \times 10^6$) produced biotechnologically *via* fermentation of bacterial strain *Streptococcus equi susp. zooepidemicus* was acquired from Contipro a.s. (Czech Republic).

Ammonium peroxydisulfate (APS; 98 %), aniline hydrochloride (AH; reagent-grade ≥ 98 %) were also acquired from Sigma Aldrich (Germany).

2.2. Preparation and characterization of films

2.2.1. *Synthesis of composite films*

Composite films were prepared *in situ* during the preparation of colloidal PANI dispersions on the various supports defined below. Tissue polystyrene culture dishes (TPP; Switzerland) was used for cytocompatibility testing, glass slides for determinations of surface energy and silicon wafers for the visualization of dried colloids by optical microscopy.

Hyaluronate and chitosan stabilized colloidal PANI was synthesized *via* the oxidation of AH with APS in the presence of each of the biopolymer according to procedure described previously in (Kasarkova et al., 2019).

For the production of films containing SH, APS (0.1 mol L^{-1}) was dissolved in water and AH (0.2 mol L^{-1}) was similarly dissolved in an aqueous solution of SH (1 wt%). A solution of stabilizing SH (1 wt%) was prepared by the SH overnight dissolution in stirred demineralized water at $55 \text{ }^\circ\text{C}$. The polymerization of AH was initiated at room temperature by mixing the solutions of AH/SH and APS. Polymerization was completed within 4 h. The resulting composite film adhered on the respective support were designated as PANI-SH.

Similar films were also prepared with CH as a stabilizer. Chitosan (2 wt%) was dissolved in 1 mol L^{-1} hydrochloric acid under the corresponding conditions for SH and the solutions were then filtered to remove any insoluble polymer residues. An aqueous APS solution (0.25 mol L^{-1}) was added to the solution containing AH (0.2 mol L^{-1}) and stabilizing CH (2 wt%). The oxidation of AH was allowed to proceed for 12 h. The films were designated as PANI-CH. As the layer of PANI-CH film was too thin ($\sim 30 \text{ nm}$), the procedure was repeated and a second layer of the film was deposited on this first layer. The final thicknesses of the films used were (125 ± 9) nm for PANI, (55 ± 5) nm for PANI-SH and (66 ± 8) nm for PANI-CH.

The supports with deposited both types of films (PANI-SH and PANI-CH) were rinsed with 0.2 M hydrochloric acid, followed by methanol, and allowed to air dry. Standard PANI films, used as a reference surfaces, were prepared in a similar manner without any stabilizer and designated as PANI.

The detailed description of characterization work is given in supplementary material (SM 2.2 and SM 2.3)

2.2.2. *Surface energy*

Contact angle measurements and determination of surface energy were conducted with the aid of a Theta Optical Tensiometer (Biolin Scientific, Finland). For all films, demineralized water, ethylene glycol, and diiodomethane (Sigma-Aldrich, Germany) were used as test liquids. The substrate surface free-energy was determined by means of the "acid–base" method.

2.2.3. *Spectroscopic characterization*

A Thermo Nicolet NEXUS 870 FTIR Spectrometer (Madison, WI 537 11, USA) in a dry air purged environment with a DTGS TEC (deuterated triglycine sulfate thermoelectric cooled) detector in the wavelength range 400 to 4000 cm^{-1} was used to measure infrared spectra. Measurements of PANI-CH and PANI-SH dispersions deposited on silicon supports were performed *ex situ* in transmission mode. Optical micrographs of the studied films deposited on a silicon window were captured using research grade Leica DM LM microscope with objective magnification 50x.

2.2.4. *Atomic force microscopy*

The surface topographies (including thickness) and electrical properties of the films were analysed by tunnelling AFM using the PeakForce TUNA module on a Dimension ICON instrument (Bruker Corporation; USA). The resulting TUNA current signals and area roughness parameters were determined according to the ISO 25178-2 standard using NanoScope Analysis software v.1.5. The following parameters were determined: (1) mean and maximum TUNA current, (2) surface roughness (Sa), and (3) maximum surface height (Sz) and (4) surface area increase (Rsa).

2.2.5. *Conductivity*

The conductivity of the films was determined by the four-point van der Pauw method. A programmable electrometer with an SMU Keithley 237 current source and a Multimeter Keithley 2010 voltmeter with a 2000 SCAN 10-channel scanner card (USA) were used. Measurements were carried out at ambient temperature. Triplicates were performed for all

samples tested. The stability of the composite films with respect to their ability to maintain conductivity was determined after their storage at ambient temperature for two months.

~~2.2.6.~~ *Stability*

2.3. Determination of biological properties

2.3.1. *Protein adsorption*

The amount of bovine serum albumine (BSA, Sigma aldrich) and vitronectin (Gibco) adsorbed on the substrates was determined using the Micro-BCA Protein Assay Kit (Thermo Scientific, USA). The absorbance of the protein solutions was measured at 562 nm with a UV-Vis Infine 200 PRO spectrometer (Tecan, Switzerland) and compared with a protein standard curve. Three replicates were performed for all tested samples.

2.3.2. *Antibacterial properties*

The antibacterial testing of the films was conducted using gram-positive *Staphylococcus aureus* CCM 4516 and gram-negative *Escherichia coli* CCM 4517 purchased from the Czech Collection of Microorganisms (Czech Republic). The antibacterial activity was determined according to the protocol of EN ISO 22196 with modifications. All the tests were run in triplicates.

2.3.3. *Cytocompatibility of hiPSC*

Cell lines and cultivation protocol: The cytocompatibilities of the films were determined using two hiPSC lines of different origins, namely, the M67 line (derived from fibroblast from a 67-year-old male that was reprogrammed by episomal vector Epi5 Epi5 (ThermoFisher) and the Neo d1 line (derived from neonatal fibroblast (Lonza) and reprogrammed by Sendai virus using Cytotune kit 1.0 (ThermoFisher). HiPSC were derived and cultured according to the protocol of the European Bank for induced pluripotent Stem Cells, as described previously (Barta et al., 2016; Renzova et al., 2018).

Adhesion, proliferation and cardiomyogenesis of hiPSC: Both used hiPSC lines were cultivated on tissue culture plastics coated with vitronectin. In all experiments the cells (10^5 cells per ml; 2 mL of cells suspension per well on six-wells plate was used) were seeded as small cell clumps, which contained approximately 3 to 10 cells. The cells were cultured in 2 ml

media per well on used six-wells plate in all mentioned experiments. The following assays were performed. At first, the adhesion of hiPSC cells was determined by microscopic observation 24 h after seeding. Then, the initial growth/proliferation of cells was determined by measuring the level of ATP in cell lysate 4 days after seeding (Konopka et al., 2010). Finally, cardiomyogenesis in hiPSC populations, based on the appearance of beating clusters and the expressions of transcripts related to the cardiomyocyte phenotype, was evaluated after 14 days of cell differentiation (Table 1). These results also serve as a measure of the embryotoxic effect.

Analysis of gene expression by qRT-PCR: Total RNA was extracted by RNeasy Mini Kit (Qiagen). Complementary DNA was synthesised using M-MLV reverse transcriptase kit (Sigma-Aldrich following the manufacturer instructions. qRT-PCR was performed in a Roche Light-cycler (Roche). HPRT1 was used as a reference gene primer sequences and probes are listed in Table 1.

Table 1. Probes and sequences of primers used in quantitative qRT-PCR

NCBI Reference Sequence	Gene		Primer sequence	UPL probe no.	Temp. (°C)
NM_004387.3	NKX2-5	F	cacctcaacagctccctga	#7	59
		R	ctaggtctccgcaggagtga		60
NM_021223.2	MYL7	F	gggtggtgaacaaggatgag	#2	60
		R	gtgtcagggcgaacatctg		60
NM_002471.3	MYH6	F	ctcaagctcatggccactct	#63	60
		R	gcctcctttgctttaccact		59
NM_000257.3	MYH7	F	catctccaaggagagacca	#73	60
		R	ccagcacatcaaagcgta		59
NM_000194.2	HPRT1	F	tgaccttgattattttgcatacc	#73	59
		R	cgagcaagacgttcagtct		60

Immunocytochemistry: Cells were washed with PBS, fixed with 4% formaldehyde solution, permeabilised by a 0.1% Triton X-100 solution in PBS, and blocked in 1% BSA in PBS. Then, the cells were incubated with anti- α -actinin antibody (Sigma-Aldrich) overnight at 4 °C. The following day, the cells were incubated with anti-mouse IgG conjugate Alexa568

(Invitrogen) for 1 h at room temperature. Nuclei were counterstained with a Draq5 (Invitrogen, USA). Images were acquired using Leica SP8 confocal microscopy (Leica Microsystems, Germany)

3. Results and discussion

3.1. Surface energy

The surface energies of PANI films prepared in the absence of stabilizing polymers were determined earlier (Humpolicek et al., 2015). The measurements from the current study show that the surface energies of the films prepared in the presence of biopolymers were different in comparison with pristine PANI films (Table 2). They differed in their values of γ^{TOT} , which were both lower for PANI-SH and PANI-CH than for PANI film without polysaccharides. Moreover, the components representing the dispersive (γ^{LW}) and polar (γ^{AB}) parts of surface energy were different for PANI-SH and PANI-CH. Here, the PANI-CH film exhibited the lowest dispersive and highest polar components of surface energy, such a combination likely to influence its biological properties.

Table 2. Contact angles determined in water, ethylene glycol (EG), and diiodomethane (DI) together with surface energy γ of pristine polyaniline (PANI) and composites (PANI-SH, PANI-CH)

Sample	Contact angles (°)			Surface energy components (mN m ⁻¹)		
	H ₂ O	EG	DI	γ^{TOT}	γ^{LW}	γ^{AB}
PANI ^{a)}	n.d.	n.d.	n.d.	52.5	46.1	6.5
PANI-SH	33.2± 2	16.2±0.2	25.3±0.4	48.3±0.1	46.0±0.1	2.2± 0.1
PANI-CH	27.1± 0.8	12.8± 1	47.2± 0.7	46.5±0.1	35.8±0.3	10.7±0.4

a) Values of surface energy adopted from (Humpolicek et al., 2015)

n.d. not determined

3.2. Spectroscopic spectroscopy

The infrared spectrum of PANI film (spectrum PANI in Fig. 1 A) exhibits a broad absorption band of polarons at wavenumbers higher than 2000 cm⁻¹, typical of the conducting form of

PANI. Absorption bands in the region 3400–2800 cm^{-1} reflect the organization of PANI chains within the film resulting from hydrogen bonding. They are connected with nitrogen-containing groups, such as the secondary amine $-\text{NH}-$ and the protonated imine $-\text{NH}^+=$.

Two main bands of quinonoid and benzenoid ring-stretching vibrations are situated at 1574 and 1497 cm^{-1} . The band observed at 1309 cm^{-1} corresponds to π -electron delocalization induced in the polymer by protonation. The band of $\text{C}\sim\text{N}^{+\bullet}$ stretching vibrations in the polaronic structure is situated at 1248 cm^{-1} . The prominent band observed at 1145 cm^{-1} reflects vibrations of the $-\text{NH}^+=$ structure. The region 900–700 cm^{-1} corresponds to aromatic ring out-of-plane deformation vibrations (Stejskal et al. Encyclopedia of Polymer Science and Technology "Conducting Polymers: Polyaniline,").

In the spectra of PANI/polysaccharide films, the main bands of PANI occur at 1574, 1497, 1309, 1248, 1145 and 812 cm^{-1} (Fig. 1, A). In the spectrum of films prepared in the presence of hyaluronate (spectrum PANI-SH in Fig. 1, A), the peaks which belong to SH are also visible; they are marked with asterisks. In addition, a peak with a maximum at 1742 cm^{-1} ($\text{C}=\text{O}$) is visible in the spectrum. In the case of stabilization with chitosan (spectrum PANI-CH in Fig. 1, A), the peaks of CH (marked with asterisks) are clearly evident. On the other hand, the peak at 1742 cm^{-1} is missing.

3.3. Optical microscopy

The optical images of films demonstrated significant differences between the PANI-CH and PANI-SH samples. While PANI-CH film is smooth with some adhering spherical colloidal particles (Fig. 1 C), in PANI-SH films fibre-like structures with green elements of protonated PANI within the shell of stabilizing polymer are observed (Fig. 1 B). This morphology can be ascribed to the presence of stabilizing SH polymer, which displays a similar fibrillar morphology also in the absence of PANI.

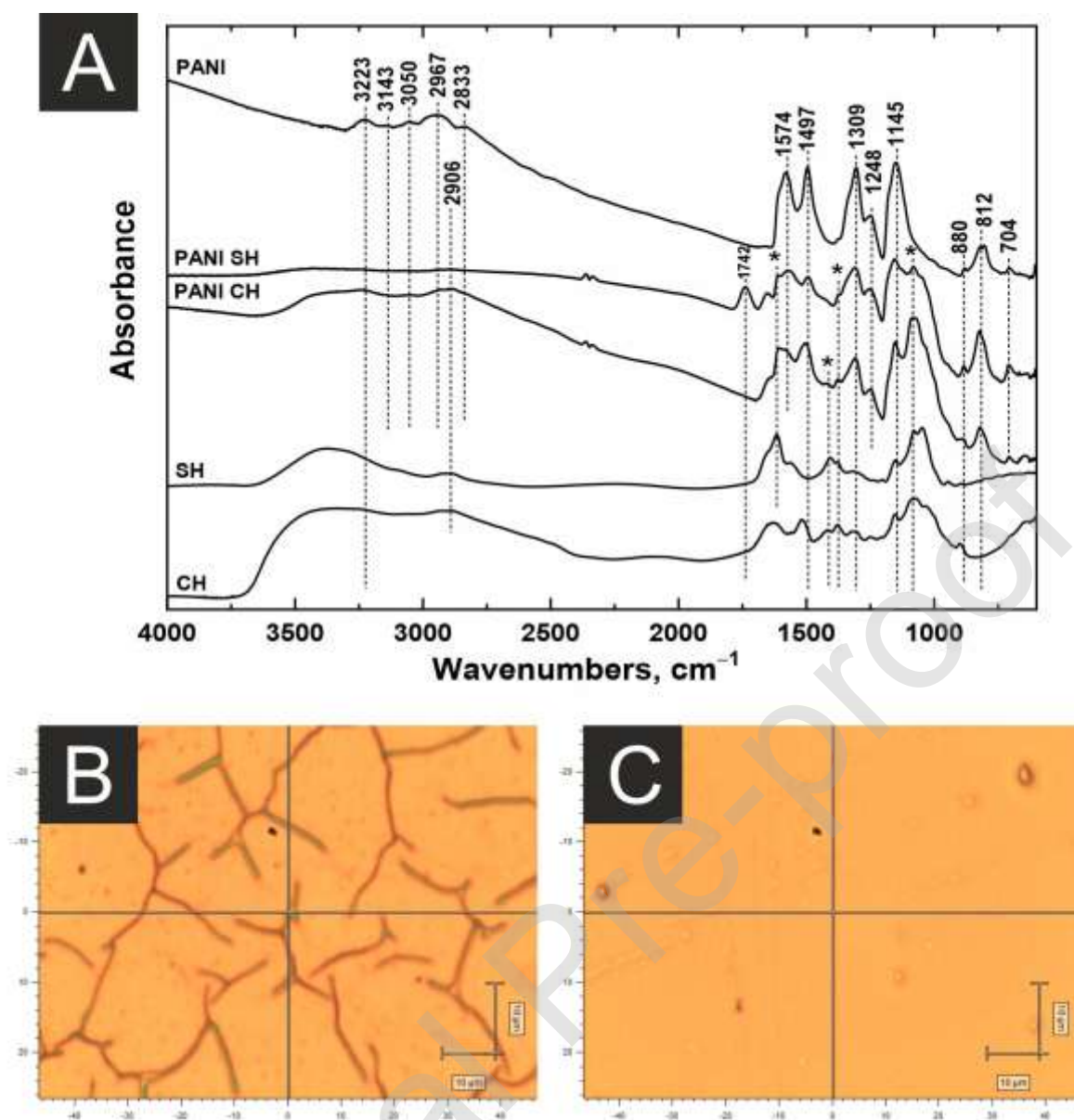
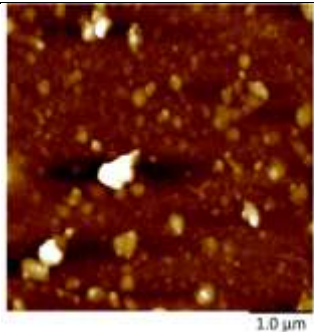
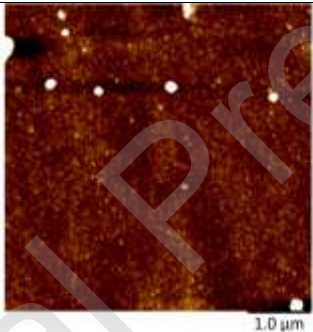
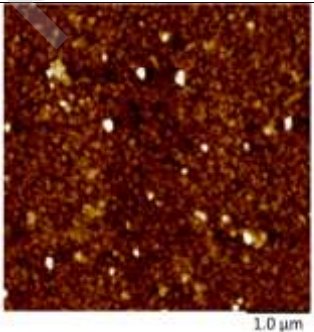
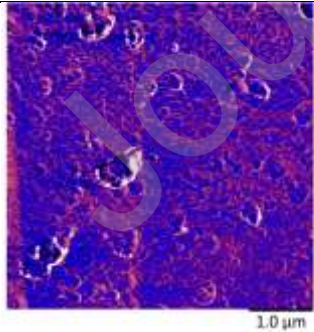
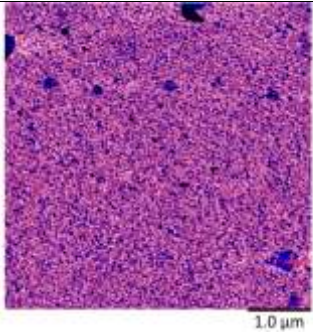
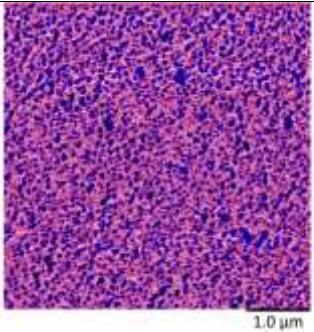


Fig. 1. Infrared spectra of pristine polyaniline (PANI) and composites (PANI-SH, PANI-CH) in comparison with hyaluronate (SH), and chitosan (CH) deposited on silicon supports (A) and optical micrographs of the films of PANI-SH (B) and PANI-CH (C) on silicon window, bar is 10 μm .

3.4. Atomic force microscopy

Cell attachment and proliferation on solid surfaces depend on a number of variables, with surface chemistry and topography playing a key role. In order to describe the surface topography of the studied films, roughness together with surface electrical properties were determined using AFM. The roughness parameters S_z , S_a and R_{sa} (Fig. 2) were

significantly different between pristine PANI (28 nm) and both biopolymer-modified films with notably smoother surfaces. Here, Sa values for PANI-SH and PANI-CH were 4 and 14 nm, respectively. Surprisingly, the SH-modified film, in which polymer of very high molecular weight was used, exhibited a rather uniform surface (Rsa , surface area increase only about 3 % from 25.0 to 25.8 μm^2). This might be due to the special morphology of the sample revealed by optical microscopy (Fig. 1 B). As already mentioned by Wang et al. (Wang, Ji, Li, & Wang, 2008), the nano-scale morphology of PANI can be a factor influencing cell adhesion. Correspondingly to roughness, differences between the samples were also observed with respect to their surface electrical properties. Specifically, the average TUNA current decreased in accordance with decreasing surface roughness in the order PANI > PANI-CH > PANI-SH with all values ranging from 24 to 5 pA. Classification of the samples from the most to the least conducting as determined by AFM is in reasonably good agreement with conductivity measurements obtained on these materials by the van der Pauw method – not, of course, in terms of absolute values of conductivity but only as regards their order.

PANI	PANI-SH	PANI-CH
		
$Sz = 577 \text{ nm}$	$Sz = 120 \text{ nm}$	$Sz = 236 \text{ nm}$
$Sa = 28 \text{ nm}$	$Sa = 4 \text{ nm}$	$Sa = 14 \text{ nm}$
$Rsa = 26 \%$	$Rsa = 3 \%$	$Rsa = 25 \%$
		
Max. TUNA current = 860 pA	Max. TUNA current = 53 pA	Max. TUNA current = 103 pA

Average TUNA current = 24 pA	Average TUNA current = 5 pA	Average TUNA current = 12 pA
---------------------------------	--------------------------------	---------------------------------

Fig. 2. AFM images pristine polyaniline (PANI) and composites (PANI-SH, PANI-CH). Top images show height changes, below TUNA current maps.

3.5. Conductivity

In comparison with composites, standard PANI films demonstrated slightly higher conductivity ($5.5 \pm 0.7 \text{ S cm}^{-1}$), which was of the same order of magnitude as the typical values reported for thin PANI films stabilized with poly(*N*-vinylpyrrolidone) ($2.6 \pm 0.7 \text{ S cm}^{-1}$) (Stejskal & Sapurina, 2005). The conductivities of composite films did not differ notably and ranged from 1.1 S cm^{-1} (PANI-SH) to 2.3 S cm^{-1} (PANI-CH). The results obviously show that the presence of polysaccharides in composites did not significantly decrease the electrical properties of the products.

3.6. Stability

It is known that neat PANI is reasonably stable toward environmental stresses, however its stability in terms of conductivity is notably influenced by temperature (Stejskal et al. Encyclopedia of Polymer Science and Technology "Conducting Polymers: Polyaniline,"). Therefore, the development of conductivity of the PANI-SH and PANI-CH was followed during their storage. The data proved good stability of the films in terms of conductivity, which did not significantly decreased after two months storage. It's values were within the same order of magnitude with values 1.5 and 1.2 S cm^{-1} for PANI-SH and PANI-CH, respectively.

3.7. Protein adsorption

After the application of biomaterials into a host body, the first interaction at the biointerface is the adsorption of proteins. The adsorption process is a multifactorial phenomenon involving a broad range of interactions, of which hydrophobic interactions, hydrogen bonding, and electrostatic interactions are mainly involved (Nakanishi, Sakiyama, & Imamura, 2001). These processes play a crucial role in subsequent reactions of cells and the immune system. The analyses of the films show that in the case of pristine PANI and PANI-SH the adsorption of BSA was twice as high as that on the reference surface (Fig. 3). In contrast,

the adsorption of BSA on films containing chitosan (PANI-CH) was comparable to the level determined on the reference. Vitronectin adsorbed best on neat PANI surface and the adsorption was significantly better than that on the reference. On the other side, the adsorption of vitronectin on composites was similar to reference, but lower than on PANI. The adsorption pattern it hence different in comparison with BSA. Looking at Figure 4, cell adhesion on vitronectin-treated films is opposite to amount of vitronectin adsorbed, and is significantly lower on neat PANI in comparison with both composites. Hence the positive effect of biocompatible polysaccharides is obvious.

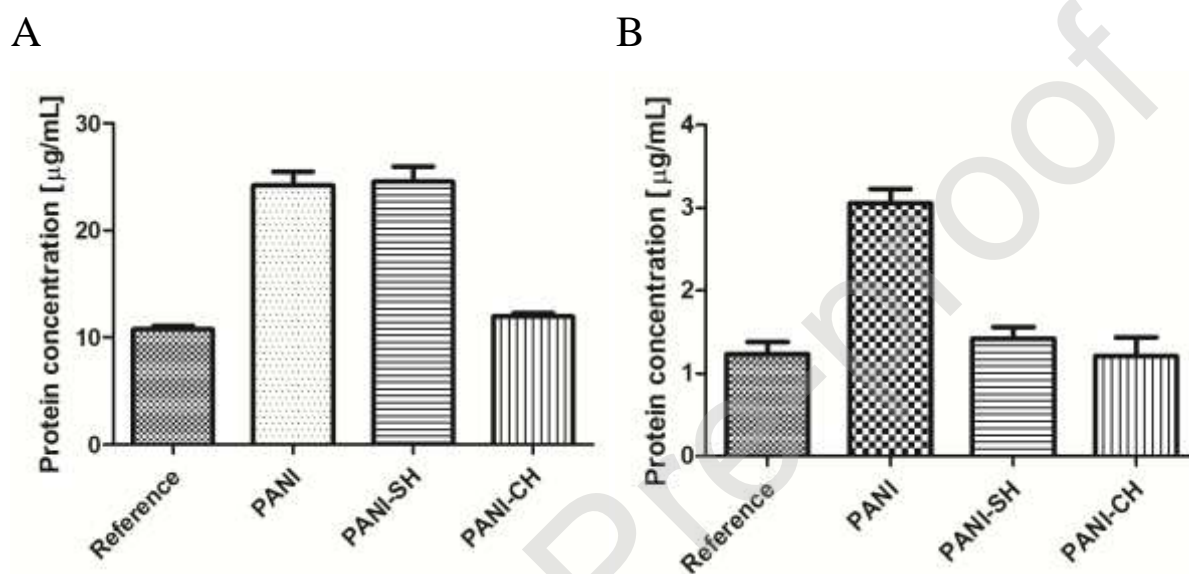
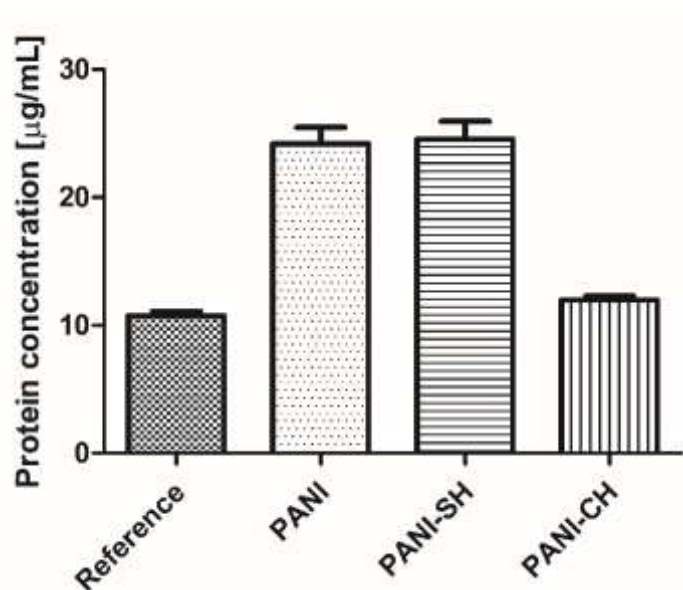


Fig. 3. The protein adsorption on pristine polyaniline (PANI) and composites (PANI-SH, PANI-CH);A) bovine serum albumin B) vitronectin



3.8. Antibacterial activity

Polyaniline itself possesses antibacterial activity, both in the form of films (Kucekova, Kasparikova, Humpolicek, Sevcikova, & Stejskal, 2013) and also colloidal dispersions (Kasparikova et al., 2019). Though the antimicrobial activity of hyaluronic acid against both bacterial and fungi species has been mentioned in literature (Ardizzoni et al., 2011; Drago et al., 2014), this polymer is not commonly considered as an antibacterial agent. On the other hand, chitosan is well known for its antibacterial action (Ma, Garrido-Maestu, & Jeong, 2017). The antibacterial activity of both biomacromolecules depends also on their conformation and molecular weight, though the correlation between molecular weight and antibacterial activity is not unambiguous. The overall antibacterial activity of the composite films described here is, therefore, likely controlled by the concentration of components (polysaccharides and PANI) as well as by changes in the conformation of biomacromolecules.

The antibacterial activity determined on two common bacterial strains (*E. Coli* and *S. aureus*) differed for pristine PANI and its composites (Table 3). Pristine PANI exhibited significant antibacterial activity toward both types of tested bacteria. PANI-SH and PANI-CH showed, however, significant antibacterial activity only against gram negative *E. coli*, and their activity against gram positive *S. aureus* was only minor. This is somewhat surprising, as gram-positive strains are usually considered to be more sensitive to the action of various antibacterial agents thanks to the composition of their cell walls. Recently, the antibacterial activity of PANI/chitosan composite was reported by Mohamadi et al (Mohammadi, Pirsas, & Alizadeh,

2019), who demonstrated the efficacy of the composite against *E. coli* and related this efficacy to the content of PANI in the film. Also, Bober et al. (Bober et al., 2017) reported on the antibacterial activity of composite films of PANI with gelatin against *S. aureus* and *E. coli*. It is therefore plausible that the antibacterial effect of composites is mainly caused by neat PANI (in the form of salt). This was shown by Kucekova et al (Kucekova et al., 2013), who demonstrated the notable impact of films composed of PANI salt on *E. coli* and *S. aureus*. However, PANI salt film failed in the suppression of biofilm-forming species of both these bacterial strains, *S. aureus* (CCM 2020, CCM 3953) and *E. coli* (CCM 3988). (Mikusova et al., 2017).

Table 3. Antibacterial activity R of pristine polyaniline (PANI) and composites (PANI-SH, PANI-CH).

Samples	Antibacterial activity R (cfu cm ⁻²)	
	<i>S. aureus</i>	<i>E. coli</i>
Reference	$U_t = 3.6 (4.6 \times 10^3)$	$U_t = 5.3 (2 \times 10^5)$
PANI	2.3 (2.0×10^1)	$\geq 5.3 (< 1)$
PANI-SH	0.2 (2.8×10^3)	$\geq 5.3 (< 1)$
PANI-CH	0.8 (6.5×10^3)	2.2 (6.0×10^3)

^a R is counted as $U_t - A_t$, where U_t and A_t is the average of the common logarithm of the number of viable bacteria (cfu cm⁻²) recovered from the reference sample and PANI films after 24 h, respectively.

3.9. Cytocompatibility

The fundamental aspects of the cytocompatibility of the studied films relate to the adhesion and initial growth and proliferation of cells on their surfaces. Here, we present the micrographs of adhered cells 24 h after seeding, and quantification of their proliferation after 4 days. The tested surfaces were pre-coated with vitronectin *prior to* cell seeding. This is a standard technique allowing for the successful seeding and survival of the hiPSC lines on any surface, including tissue culture plastics (TCP). In accordance with the behaviour of these lines on TCP, cells were not able to adhere or proliferate on the tested surfaces without coating with vitronectin.

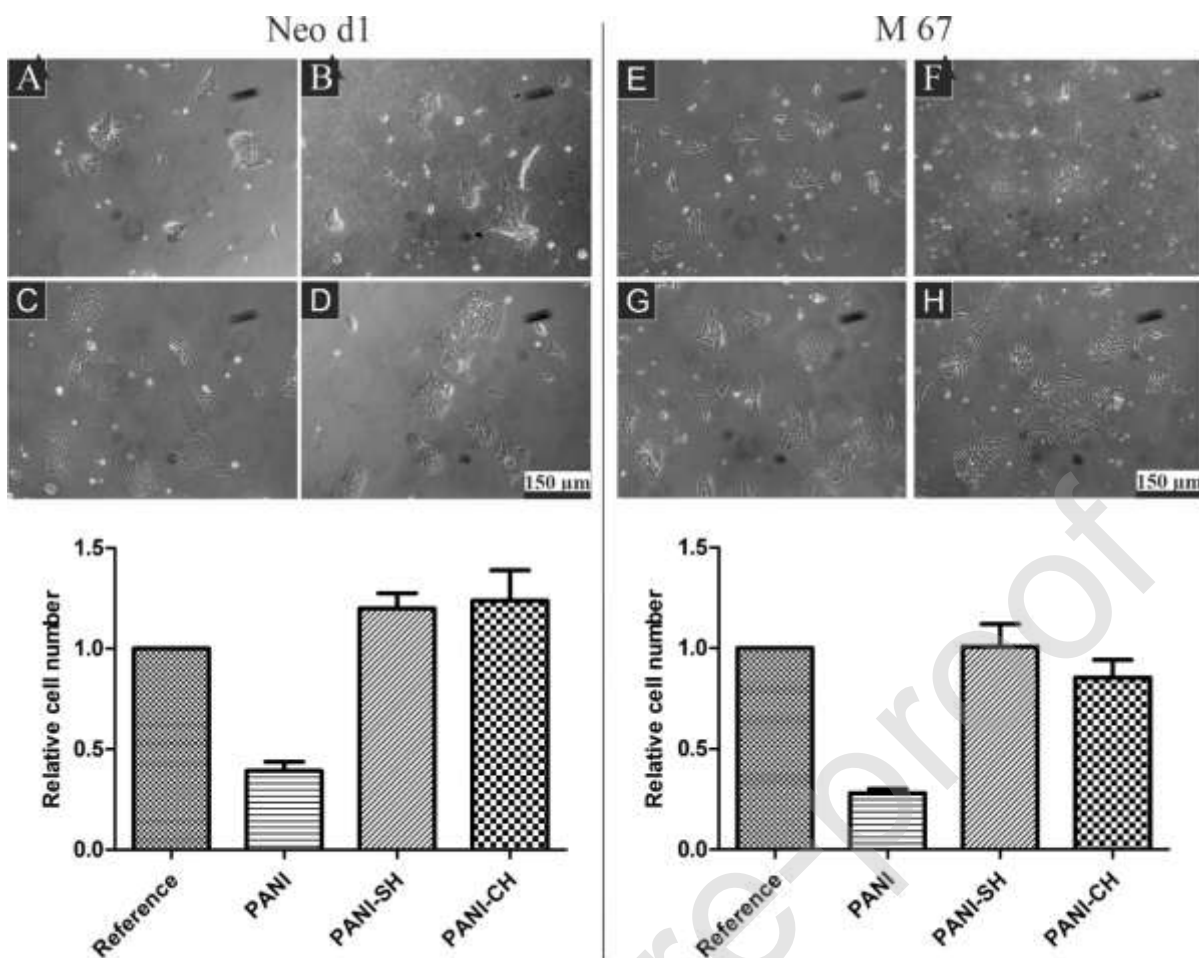


Fig. 4. The adhesion of hiPSC determined one day after seeding (micrographs A–H), which shows the morphology of adhered cells together with the quantification of initial growth/proliferation by determination of ATP level four days after seeding. hiPSC Neo d1: (A) Reference - tissue culture plastic; (B) PANI; (C) PANI-SH; (D) PANI-CH and hiPSC M67: (E) Reference; (F) PANI; (G) PANI-SH; (H) PANI-CH.

The adhesion of hiPSC determined after one day of cultivation is presented in Fig. 4. From the micrographs it is clear that both used cell lines were able to adhere on the studied surfaces and on the reference (TCP) in a comparable manner. The cells also demonstrated similar morphology. The quantification of the number of cells after 4 days of cultivation showed more interesting results (see graphs within Fig. 4). Clearly, PANI significantly decreased the cell proliferation compared to both reference TCP and PANI-SH and PANI-CH composite films. Interestingly, the proliferations of both lines on the composites were comparable to TCP, and, in the case of Neo d1, even better than on TCP. We can, therefore, conclude that none of

the composite films negatively influenced initial cell adhesion and proliferation. Although the surfaces in question allowed for cell adhesion and proliferation in the short-term experiments, undesired effects could be induced when the cells are in contact with a surface for a longer period of time.

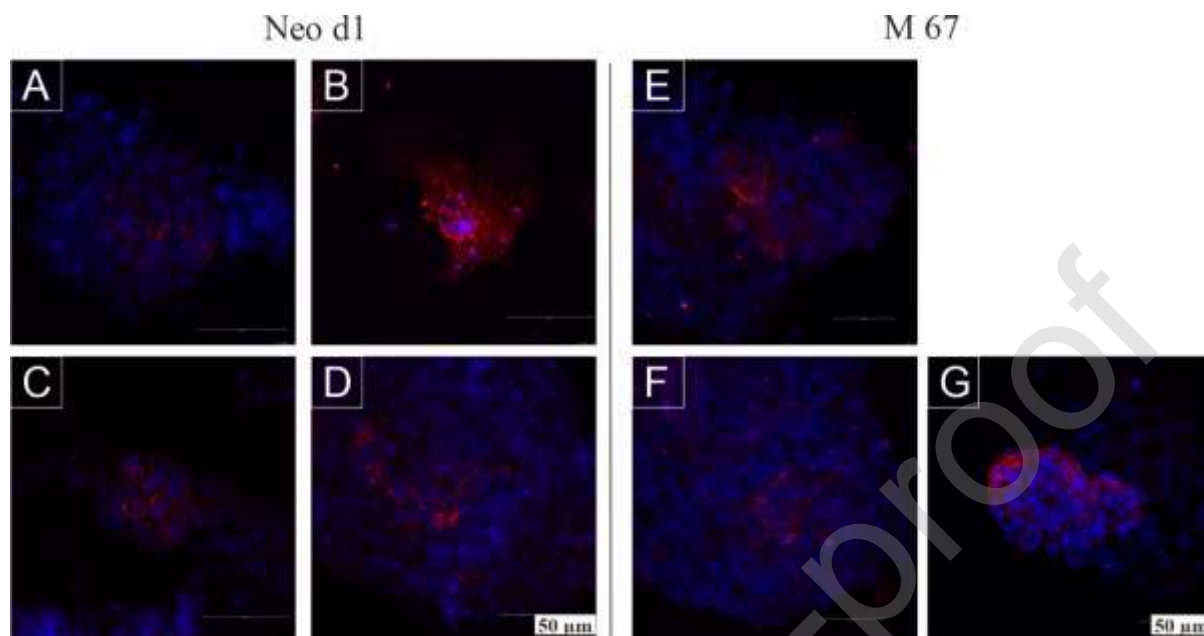


Fig. 5. Microphotographs of hiPSC after 17 days of cultivation observed by confocal microscopy. The presence of α -actinin (red) confirmed the presence of cardiomyocytes. Line NEO d1: (A) Reference - tissue culture plastic; (B) PANI; (C) PANI-SH; (D) PANI-CH. Line M 67: (E) Reference, tissue culture plastics; (F) PANI-SH; (G) PANI-CH. Cell nuclei were counterstained with Draq5; the cytoskeleton was counterstained with α -actinin.

Within the population of hiPSC, various cell lineages can be formed. The used differentiation protocol, however, leads primarily to cardiomyogenesis and this is accompanied by the appearance of spontaneously beating clusters of immature cardiomyocytes (Radaszkiewicz et al., 2016). These beating clusters were observed on both composite films but not on pristine PANI (see attached video). This is conclusive evidence that the tested composite surfaces do not exhibit embryotoxic effects. The presence of cardiomyocytes was also determined using immunohistochemical analysis. In Fig. 5, cells positive to cardiomyocyte-specific sarcomeric α -actinin are shown within the whole cell population. Cells of the M67 line were not able to grow and differentiate on PANI surfaces at all; also, Neo d1 cells were strongly reduced in number on the PANI surface, though rare colonies also containing cardiomyocytes were detected (Fig. 5). On the composite films PANI-SH and PANI-CH, the presence of

cardiomyocytes was comparable to the reference. This is further evidence of the cytocompatibility of the tested composites.

The proportion of cardiomyocytes in the total cell population can, however, vary, even due to external stimuli exerted during their growth. Cardiomyocyte proportion can be detected by the expression of cardiomyocyte-specific transcripts. First, the expression of transcription factor Nkx2.5, which determines the presence of cardiomyocytes, was detected (Hsiao et al., 2008; Radaszkiewicz et al., 2017). The expression of Nkx2.5 corresponded to the numbers of cardiomyocytes forming within the populations of the hiPSC lines. Here, we present the relative value of the mRNA expression of Nkx2.5 determined after 14 days of differentiation. In the case of the Neo d1 line, the number of forming cardiomyocytes was comparable for all studied surfaces including the reference. In contrast, the differentiation of the M67 line was highly influenced by surface characteristics. The surface of pristine PANI induced the death of the M67 line after long-term interaction (see Fig. 7), while, on the composites containing the stabilizing biopolymers PANI-SH and PANI-CH, cardiomyogenesis was greater in the population of M67 cells than on the reference material. Especially in the case of PANI-CH the proportion of cells differentiating into cardiomyocytes was significantly greater than in case of the reference.

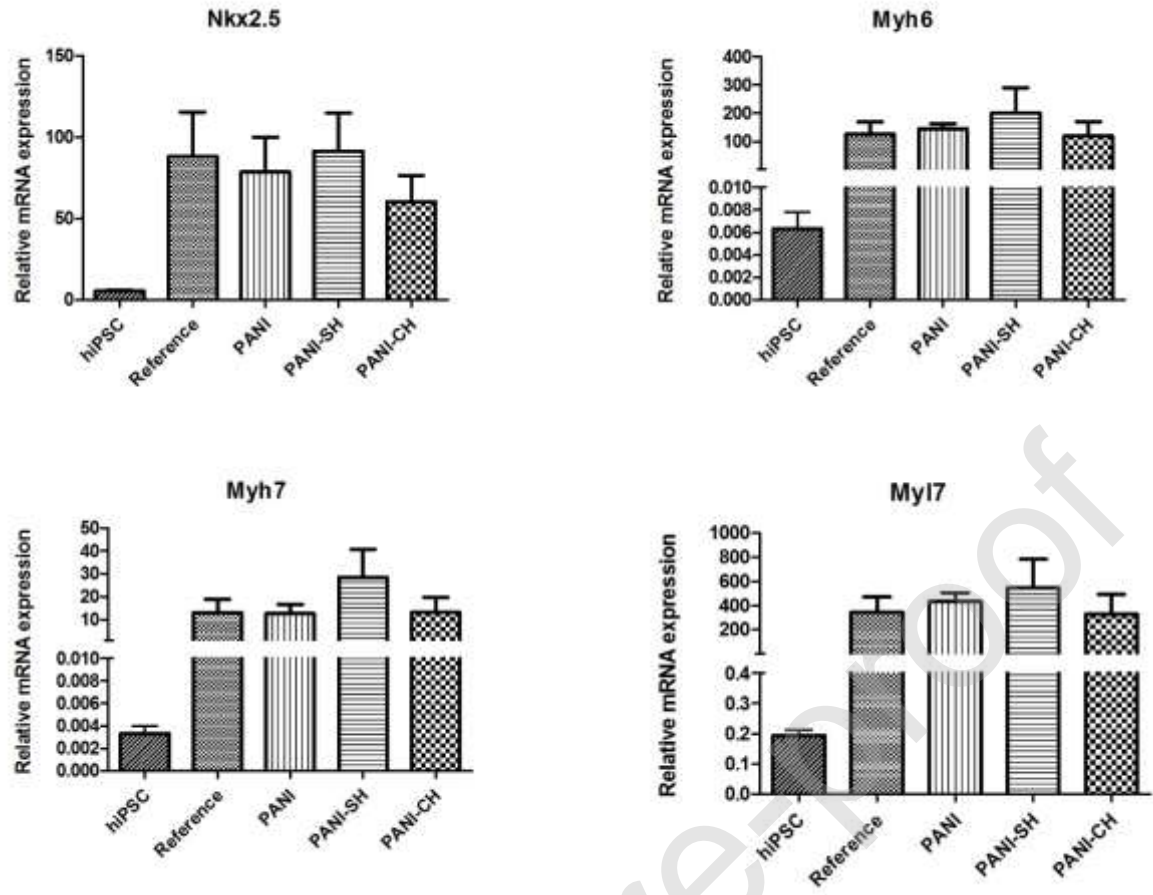


Fig. 6. Relative gene expressions of cardiomyocyte-specific transcripts determined on hiPSC line Neo d1 after 14 days of differentiation.

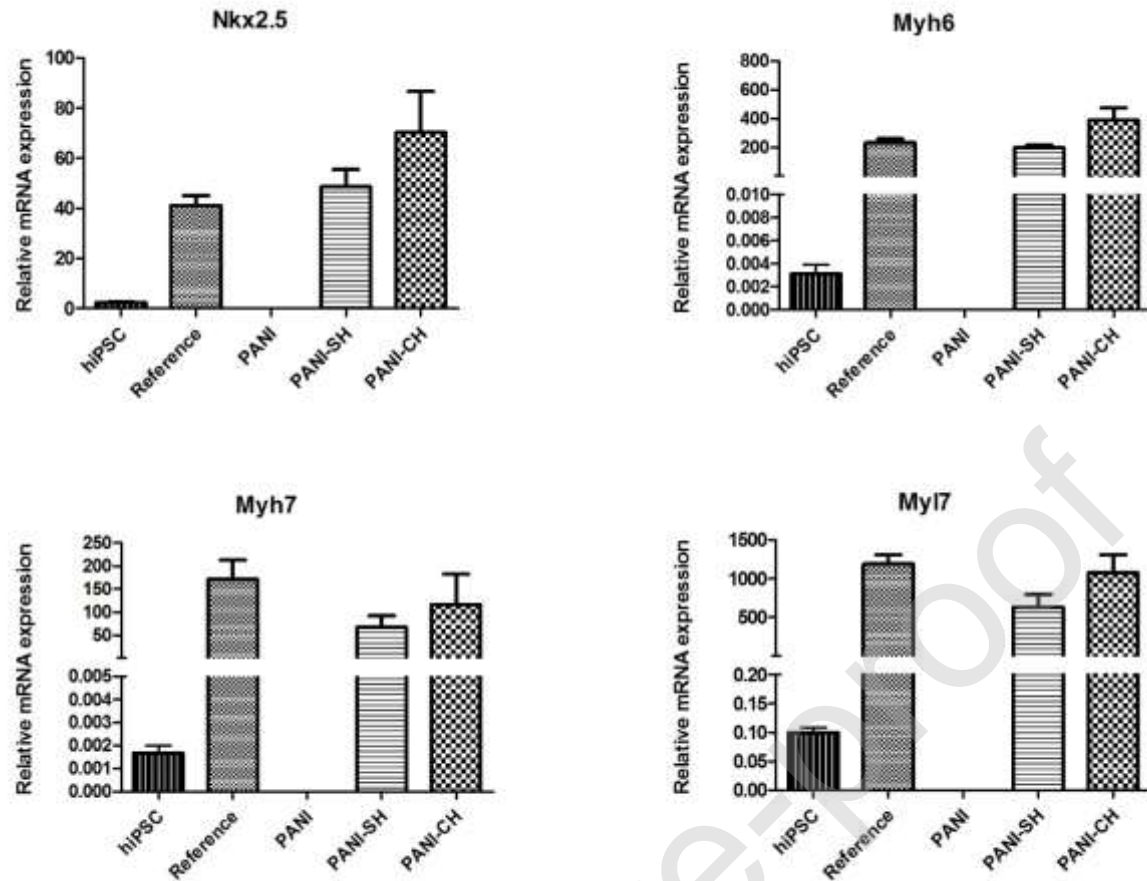


Fig. 7. Relative gene expressions of cardiomyocyte-specific transcripts determined on hiPSC line M67 after 14 days of differentiation.

Finally, the expressions of the cardiomyocyte-specific transcripts Myh6, Myh7, and Myl7 were analysed in differentiating cells (Fig. 6 and 7). Similarly to Nkx 2.5, only insignificant differences in the expressions of particular cardiomyocyte-specific transcripts were observed between the used cell lines of hiPSC. Moreover, this can be mediated even by the variability between the used hiPSC lines (Ortmann & Vallier, 2017).

4. Conclusion

Advanced composite films of conducting polyaniline (PANI) and biocompatible polysaccharides, sodium hyaluronate (SH) or chitosan (CH), were prepared by deposition on supports immersed in reaction mixture during dispersion polymerization of aniline stabilized

with the biocompatible polysaccharides. The physicochemical testing revealed that the presence of polysaccharides did not decrease the conductivity of the films in comparison with neat PANI. It modified, however, their surface energies and topography, which could influence the biological properties of the films.

The main novelty and scientific contribution of the study rests in the comprehensive investigation of biological properties of composite films. The tests have demonstrated the ability of proteins to adsorb onto their surfaces. The PANI-SH films also exhibited excellent antibacterial activity towards the common gram-negative spoilage specie *E. coli*. The present study provides clear evidence of the unique properties of composite films in terms of their cytocompatibility with HiPSCs. Both used cell lines (Neod1 and M67) were able to adhere and proliferate on the tested surfaces, at least comparably to the reference material. The differentiation protocol led to cardiomyogenesis accompanied by the formation on these films of spontaneously beating clusters of cardiomyocytes. The presence of cardiomyocytes was also confirmed by immunohistochemistry through the detection of cells positive to cardiomyocyte-specific sarcomeric α -actinin within cells growing on the films. As the presence of beating clusters is one of the markers of the absence of embryotoxicity, it can also be concluded that the films do not induce embryotoxic effects.

In summary, the immobilization of PANI/polysaccharide films at various supports using conducting polyaniline chemistry affords an elegant way how to prepare functional surfaces for the biochemical applications. The novel composite films exhibited a range of outstanding properties, mainly including excellent cytocompatibility, the absence of embryotoxicity, and reasonably high conductivity, the latter being comparable with pristine polyaniline.

Credit Author Statement

Conceptualization: Petr Humpolíček, Věra Kašpárková, Zdenka Capáková

Methodology: Petr Humpolíček, Věra Kašpárková, Zdenka Capáková, Jiří Pacherník, Jaroslav Stejskal

Investigation: Daniela Jasenská, Katarzyna Anna Radaszkiewicz, Zdenka Capáková, Jiří Pacherník, Miroslava Trchová, Antonín Minařík, Jan Vajd'ák, Tomáš Bárta, Marián Lehocký, Thanh Huong Truong, Robert Moučka

Acknowledgement

This work was supported by the Czech Science Foundation (19-16861S) and by the Ministry of Education, Youth and Sports of the Czech Republic (NPU I, LO1504). Two of the authors (K.A.R. and T.B.) gratefully acknowledge support from the Czech Science Foundation (18-18235S). D.J., J. V. and T.H.T. thank for the support from Tomas Bata University in Zlin (IGA/CPS/2020/001).

References

- Ardizzoni, A., Neglia, R. G., Baschieri, M. C., Cermelli, C., Caratozzolo, M., Righi, E., . . . Blasi, E. (2011). Influence of hyaluronic acid on bacterial and fungal species, including clinically relevant opportunistic pathogens. *Journal of Materials Science-Materials in Medicine*, 22(10), 2329-2338. doi:10.1007/s10856-011-4408-2
- Barta, T., Peskova, L., Collin, J., Montaner, D., Neganova, I., Armstrong, L., & Lako, M. (2016). Brief Report: Inhibition of miR-145 Enhances Reprogramming of Human Dermal Fibroblasts to Induced Pluripotent Stem Cells. *Stem Cells*, 34(1), 246-251. doi:10.1002/stem.2220
- Bober, P., Humpolicek, P., Syrovy, T., Capakova, Z., Syrova, L., Hromadkova, J., & Stejskal, J. (2017). Biological properties of printable polyaniline and polyaniline-silver colloidal dispersions stabilized by gelatin. *Synthetic Metals*, 232, 52-59. doi:10.1016/j.synthmet.2017.07.013
- Chattopadhyay, D., Banerjee, S., Chakravorty, D., & Mandal, B. M. (1998). Ethyl(hydroxyethyl)cellulose stabilized polyaniline dispersions and destabilized nanoparticles therefrom. *Langmuir*, 14(7), 1544-1547. doi:10.1021/la970936u
- . Conducting Polymers: Polyaniline. In *Encyclopedia of Polymer Science and Technology* (pp. 1-44).
- Drago, L., Cappelletti, L., De Vecchi, E., Pignataro, L., Torretta, S., & Mattina, R. (2014). Antiadhesive and antibiofilm activity of hyaluronic acid against bacteria responsible for respiratory tract infections. *Apmis*, 122(10), 1013-1019. doi:10.1111/apm.12254
- Fernandez, T. D., Fernandez, C. D., & Mencalha, A. L. (2013). Human Induced Pluripotent Stem Cells from Basic Research to Potential Clinical Applications in Cancer. *Biomed Research International*, 11. doi:10.1155/2013/430290
- Hsiao, E. C., Yoshinaga, Y., Nguyen, T. D., Musone, S. L., Kim, J. E., Swinton, P., . . . Conklin, B. R. (2008). Marking Embryonic Stem Cells with a 2A Self-Cleaving Peptide: A NKX2-5 Emerald GFP BAC Reporter. *Plos One*, 3(7), 8. doi:10.1371/journal.pone.0002532
- Hu, M., Sabelman, E. E., Tsai, C., Tan, J., & Hentz, V. R. (2000). Improvement of schwann cell attachment and proliferation on modified hyaluronic acid strands by polylysine. *Tissue Engineering*, 6(6), 585-593. doi:10.1089/10763270050199532
- Humpolicek, P., Radaszkiewicz, K. A., Kasparkova, V., Stejskal, J., Trchova, M., Kucekova, Z., . . . Minarik, A. (2015). Stem cell differentiation on conducting polyaniline. *Rsc Advances*, 5(84), 68796-68805. doi:10.1039/c5ra12218j
- Kasparkova, V., Jasenska, D., Capakova, Z., Marakova, N., Stejskal, J., Bober, P., . . . Humpolicek, P. (2019). Polyaniline colloids stabilized with bioactive polysaccharides:

- Non-cytotoxic antibacterial materials. *Carbohydrate Polymers*, 219, 423-430. doi:10.1016/j.carbpol.2019.05.038
- Kirker, K. R., Luo, Y., Nielson, J. H., Shelby, J., & Prestwich, G. D. (2002). Glycosaminoglycan hydrogel films as bio-interactive dressings for wound healing. *Biomaterials*, 23(17), 3661-3671. doi:10.1016/s0142-9612(02)00100-x
- Kucekova, Z., Kasparikova, V., Humpolicek, P., Sevcikova, P., & Stejskal, J. (2013). Antibacterial properties of polyaniline-silver films. *Chemical Papers*, 67(8), 1103-1108. doi:10.2478/s11696-013-0385-x
- Lapcik, L., De Smedt, S., Demeester, J., & Chabreck, P. (1998). Hyaluronan: Preparation, structure, properties, and applications. *Chemical Reviews*, 98(8), 2663-2684. doi:10.1021/cr941199z
- Liu, Y., Yin, P. F., Chen, J. R., Cui, B., Zhang, C., & Wu, F. (2020). Conducting Polymer-Based Composite Materials for Therapeutic Implantations: From Advanced Drug Delivery System to Minimally Invasive Electronics. *International Journal of Polymer Science*, 2020. doi:10.1155/2020/5659682
- Ma, Z. X., Garrido-Maestu, A., & Jeong, K. C. (2017). Application, mode of action, and in vivo activity of chitosan and its micro and nanoparticles as antimicrobial agents: A review. *Carbohydrate Polymers*, 176, 257-265. doi:10.1016/j.carbpol.2017.08.082
- Machalowski, T., Wysokowski, M., Zoltowska-Aksamitowska, S., Bechmann, N., Binnewerg, B., Schubert, M., . . . Ehrlich, H. (2019). Spider Chitin. The biomimetic potential and applications of Caribena versicolor tubular chitin. *Carbohydrate Polymers*, 226, 11. doi:10.1016/j.carbpol.2019.115301
- Maciel, B. G., da Silva, R. J., Chavez-Guajardo, A. E., Medina-Llamas, J. C., Alcaraz-Espinoza, J. J., & de Melo, C. P. (2018). Magnetic extraction and purification of DNA from whole human blood using a gamma-Fe₂O₃@Chitosan@Polyaniline hybrid nanocomposite. *Carbohydrate Polymers*, 197, 100-108. doi:10.1016/j.carbpol.2018.05.034
- Mikusova, N., Humpolicek, P., Ruzicka, J., Capakova, Z., Janu, K., Kasparikova, V., . . . Ponizil, P. (2017). Formation of bacterial and fungal biofilm on conducting polyaniline. *Chemical Papers*, 71(2), 505-512. doi:10.1007/s11696-016-0073-8
- Mohammadi, B., Pirsa, S., & Alizadeh, M. (2019). Preparing chitosan-polyaniline nanocomposite film and examining its mechanical, electrical, and antimicrobial properties. *Polymers & Polymer Composites*, 27(8), 507-517. doi:10.1177/0967391119851439
- Nakanishi, K., Sakiyama, T., & Imamura, K. (2001). On the adsorption of proteins on solid surfaces, a common but very complicated phenomenon. *Journal of Bioscience and Bioengineering*, 91(3), 233-244. doi:10.1263/jbb.91.233
- Ortmann, D., & Vallier, L. (2017). Variability of human pluripotent stem cell lines. *Current Opinion in Genetics & Development*, 46, 179-185. doi:10.1016/j.gde.2017.07.004
- Ozkan, O., & Sasmazel, H. T. (2018). Antibacterial Performance of PCL-Chitosan Core-Shell Scaffolds. *Journal of Nanoscience and Nanotechnology*, 18(4), 2415-2421. doi:10.1166/jnn.2018.14378
- Paulsen, B. D., Tybrandt, K., Stavrinidou, E., & Rivnay, J. (2020). Organic mixed ionic-electronic conductors. *Nature Materials*, 19(1), 13-26. doi:10.1038/s41563-019-0435-z
- Qin, Q., Tao, J., & Yang, Y. (2010). Preparation and characterization of polyaniline film on stainless steel by electrochemical polymerization as a counter electrode of DSSC. *Synthetic Metals*, 160(11-12), 1167-1172. doi:10.1016/j.synthmet.2010.03.003

- Radaszkiewicz, K. A., Sykorova, D., Bino, L., Kudova, J., Bebarova, M., Prochazkova, J., . . . Pachernik, J. (2017). The acceleration of cardiomyogenesis in embryonic stem cells in vitro by serum depletion does not increase the number of developed cardiomyocytes. *Plos One*, *12*(3), 17. doi:10.1371/journal.pone.0173140
- Radaszkiewicz, K. A., Sykorova, D., Karas, P., Kudova, J., Kohut, L., Bino, L., . . . Pachernik, J. (2016). Simple non-invasive analysis of embryonic stem cell-derived cardiomyocytes beating in vitro. *Review of Scientific Instruments*, *87*(2). doi:10.1063/1.4941776
- Renzova, T., Bohaciakova, D., Esner, M., Pospisilova, V., Barta, T., Hampl, A., & Cajanek, L. (2018). Inactivation of PLK4-STIL Module Prevents Self-Renewal and Triggers p53-Dependent Differentiation in Human Pluripotent Stem Cells. *Stem Cell Reports*, *11*(4), 959-972. doi:10.1016/j.stemcr.2018.08.008
- Riede, A., Helmstedt, M., Riede, V., Zemek, J., & Stejskal, J. (2000). In situ polymerized polyaniline films. 2. Dispersion polymerization of aniline in the presence of colloidal silica. *Langmuir*, *16*(15), 6240-6244. doi:10.1021/la991414c
- Riede, A., Helmstedt, M., Sapurina, I., & Stejskal, J. (2002). In situ polymerized polyaniline films 4. Film formation in dispersion polymerization of aniline. *Journal of Colloid and Interface Science*, *248*(2), 413-418. doi:10.1006/jcis.2001.8197
- Stejskal, J., & Gilbert, R. G. (2002). Polyaniline. Preparation of a conducting polymer (IUPAC technical report). *Pure and Applied Chemistry*, *74*(5), 857-867. doi:10.1351/pac200274050857
- Stejskal, J., & Sapurina, I. (2005). Polyaniline: Thin films and colloidal dispersions - (IUPAC technical report). *Pure and Applied Chemistry*, *77*(5), 815-826. doi:10.1351/pac200577050815
- Stejskal, J., Sapurina, I., Prokes, J., & Zemek, J. (1999). In-situ polymerized polyaniline films. *Synthetic Metals*, *105*(3), 195-202. doi:10.1016/s0379-6779(99)00105-8
- Stejskal, J., Sapurina, I., & Trchova, M. (2010). Polyaniline nanostructures and the role of aniline oligomers in their formation. *Progress in Polymer Science*, *35*(12), 1420-1481. doi:10.1016/j.progpolymsci.2010.07.006
- Stejskal, J., Spirkova, M., Riede, A., Helmstedt, M., Mokreva, P., & Prokes, J. (1999). Polyaniline dispersions 8. The control of particle morphology. *Polymer*, *40*(10), 2487-2492. doi:10.1016/s0032-3861(98)00478-9
- Thanpicha, T., Sirivat, A., Jamieson, A. M., & Rujiravanit, R. (2006). Preparation and characterization of polyaniline/chitosan blend film. *Carbohydrate Polymers*, *64*(4), 560-568. doi:10.1016/j.carbpol.2005.11.026
- Uluturk, C., & Alemdar, N. (2018). Electroconductive 3D polymeric network production by using polyaniline/chitosan-based hydrogel. *Carbohydrate Polymers*, *193*, 307-315. doi:10.1016/j.carbpol.2018.03.099
- Wang, H. J., Ji, L. W., Li, D. F., & Wang, J. Y. (2008). Characterization of nanostructure and cell compatibility of polyaniline films with different dopant acids. *Journal of Physical Chemistry B*, *112*(9), 2671-2677. doi:10.1021/jp0750957
- Wnek, G. E. E., Bowlin, G. L. (2004). Encyclopedia of Biomaterials and Biomedical Engineering. . In: Boca Raton: CRC Press.
- Zare, E. N., Makvandi, P., Ashtari, B., Rossi, F., Motahari, A., & Perale, G. (2020). Progress in Conductive Polyaniline-Based Nanocomposites for Biomedical Applications: A Review. *Journal of Medicinal Chemistry*, *63*(1), 1-22. doi:10.1021/acs.jmedchem.9b00803